Dalton Transactions

Cite this: *Dalton Trans.*, 2012, **41**, 219

www.rsc.org/dalton

PAPER

Facile *in situ* synthesis of nanofluids based on ionic liquids and copper oxide clusters and nanoparticles†

Małgorzata Swadźba-Kwaśny,* Léa Chancelier, Shieling Ng, Haresh G. Manyar, Christopher Hardacre and Peter Nockemann*

Received 22nd August 2011, Accepted 4th October 2011
DOI: 10.1039/c1dt11578b

Two stable nanofluids comprising of mixed valent copper(I,II) oxide clusters (<1 nm) suspended in 1-butyl-3-methylimidazolium acetate, [C_4mim][OAc], and copper(II) oxide nanoparticles (<50 nm) suspended in trioctyl(dodecyl)phosphonium acetate, [$P_{8\,8\,8\,12}$][OAc], were synthesised in a facile one-pot reaction from solutions of copper(II) acetate hydrate in the corresponding ionic liquids. Formation of the nanostructures was studied using ^{13}C NMR spectroscopy and differential scanning calorimetry (DSC). From a solution of $Cu(OAc)_2$ in 1-ethyl-3-methylimidazolium acetate, [C_2mim][OAc], crystals were obtained that revealed the structure of $[C_2mim][Cu_3(OAc)_5(OH)_2(H_2O)]\cdot H_2O$, indicating the formation of copper hydroxo-clusters in the course of the reaction. Synthesised nanostructures were studied using transmission electron microscopy (TEM) and X-ray photoelectron spectroscopy (XPS). Physical properties of the prepared IL-nanofluids were examined using IR and UV-VIS spectroscopy, thermogravimetric analysis (TGA), differential scanning calorimetry (DSC) and densitometry.

Introduction

Nanofluids are a relatively new class of soft materials, comprising of stable suspensions of nanometre-sized particles in fluids like water, organic solvents or ethylene glycol.[1] It has been demonstrated that suspending even a small amount of nanoparticles causes a considerable increase of the thermal conductivity of the liquid. Such nanofluids have been applied as magnetic fluids[2] and lubricants,[3] and used for the conservation of artworks.[4] Furthermore, these nanocomposite materials are under investigation as luminescent materials,[5] as novel electrolytes for batteries[6] and as potential materials for solar cell applications.[7] Finally, nanofluids have been considered as solvents and catalysts in a number of reactions.[8]

Ionic liquids (ILs) are compounds comprised exclusively of ions, usually a bulky organic cation and an organic or inorganic anion.[9] Because of their entirely ionic nature, they commonly have a very large liquidus range and an extremely low vapour pressure. Since there are millions of possible anion/cation combinations,[10] the properties of ionic liquids can be tailored, whereupon they are also referred to as 'designer solvents'.[11]

Ionic liquids have been widely applied as electrolytes, due to their high ionic conductivity and a large electrochemical window,[12] and as solvents and/or catalysts, owing to their capability to dissolve a range of solutes, especially catalytic complexes.[13] More recently, they have attracted significant interest from material scientists, as promising thermal fluids,[14] lubricants[15] and components of novel composite materials: luminescent ionogels,[16] highly conducting elastic polymers[17] or so-called buckygels.[18] Already known to be useful solvents for inorganic synthesis,[19] ionic liquids have gained an interest as ionothermal solvents[20] and templating agents for preparation of inorganic nanomaterials.[21] Since nanoparticles in solutions are only kinetically stable, they have to be stabilised against aggregation, which can be achieved by electrostatic or steric protection.[22] Ionic liquids, initially applied to take advantage of their high thermal stability and ability to dissolve inorganic materials,[23] were soon found to act as capping agents[24] and to stabilise nanoparticles against aggregation.[25]

The combination of the properties of ionic liquids and nanoparticles in the form of IL-nanofluids impart certain additional or optimised properties to ionic liquids. For example, the use of colloidal self-assembly of inorganic nanomaterials in ionic liquids for dye-sensitised solar cells (DSSCs) has been reported.[26] Lunstroot *et al.* described luminescent dispersions of lanthanide-doped LaF_3:Ln^{3+} (Ln = Eu, Nd) nanocrystals in ionic liquids.[5] Watanabe *et al.* demonstrated the long-term colloidal stability of ionic liquid-based suspensions of PMMA-grafted silica particles.[27] Photoluminescence of stable CdTe semiconductor nanoparticle dispersions in ionic liquids was accomplished by Nakashima *et al.*,[28] while magnetorheological fluids with dispersions of magnetic Fe_2O_3 nanoparticles in ionic liquids have been reported by Schubert and co-workers.[2] Recently, the synthesis of stable dispersions of Fe_3C[29] and NiO[30] nanoparticles in ionic liquids have been reported, with the ionic liquid acting as templating and stabilising agent. An enhanced electrical conductivity was

QUILL/School of Chemistry and Chemical Engineering, The Queen's University of Belfast, Belfast, BT9 5AG, United Kingdom. E-mail: m.swadzba-kwasny@qub.ac.uk, p.nockemann@qub.ac.uk

† CCDC reference number 839595. For crystallographic data in CIF or other electronic format see DOI: 10.1039/c1dt11578b

achieved by introducing copper metal nanoparticles into an imidazolium ionic liquid,[31] whereas an enhancement in thermal conductivity was gained by dispersing carbon nanotubes in the ionic liquids.[32]

Metal oxide nanoparticles have numerous applications[33] and nanosized CuO in particular has applications as material in solar cells, in gas sensing, as magnetic storage media,[34] in nanodevices,[35] for heterogeneous catalysis,[36] and as a superconductor.[37] Synthetic routes to CuO nanostructures, with ionic liquids as templating agents, were explored by Taubert and co-workers[38] and Liu *et al.*,[39] who used ionic liquid-assisted aqueous methods. Furthermore, Mudring and co-workers[40] prepared CuO nanorods in 1-butyl-3-methylimidazolium bistriflamide, with the aid of a strong base and sonication.

The purpose of this study was to produce stable IL-nanofluids in a simple, inexpensive and reproducible manner. We aimed at a one-pot synthesis in a neat ionic liquid, with no additives except for the source of copper. Thus, highly stable dispersions of CuO nanoparticles or Cu_2O clusters in ionic liquids based on acetate anion were prepared. Furthermore, the mechanism of their formation has been studied, and their physical properties were investigated.

Experimental

Trioctylphosphine was obtained from Cytec. All other chemicals were purchased from Sigma-Aldrich. Trioctyl(dodecyl)phosphonium acetate, $[P_{8\,8\,8\,12}][OAc]$, and 1-butyl-3-methylimidazolium acetate, $[C_4mim][OAc]$, were synthesised as described elsewhere.[41]

Synthesis

IL-nanofluids. A stock solution of copper(II) acetate hydrate (1.603 g, 8.029×10^{-3} mol) in $[C_4mim][OAc]$ (32.001 g, 0.1614 mol) was prepared by alternating: magnetic stirring and sonication in an ultrasound bath (*ca.* 5 h, 50 °C). A stock solution of copper(II) acetate hydrate (0.471 g, 2.359×10^{-3} mol) in $[P_{8\,8\,8\,12}][OAc]$ (9.355 g, 0.01562 mol) was prepared by alternating: magnetic stirring and sonication in an ultrasound bath (*ca.*3 h, 30 °C). From each solution, two samples were poured into sample vials, and placed in a heating block pre-heated to 120 °C. One sample of each solution was stirred using a magnetic stirrer, while the other was treated with ultrasound (Misonix 3000 ultrasound probe with a microtip). All reactions were terminated after 30 min. Subsequently, the IL-nanofluids were dried under high vacuum (60 °C, overnight), transferred to a nitrogen-filled glovebox (MBraun LabMaster dp; 0.1 ppm < O_2 and H_2O), and stored there.

Characterisation

NMR spectroscopy. Routine tests of synthesised ionic liquids (^1H and ^{13}C NMR spectroscopy) were carried out using a Bruker Avance DPX 300 spectrometer at 27 °C, using deuterated acetone as a solvent. Further experiments involved monitoring reactions carried out *in situ* in a NMR tube. Neat reaction mixtures (with d_6-dimethylsulfoxide in a sealed capillary tube as a lock) were tested by ^{13}C NMR spectroscopy at a range of temperatures, using a Bruker Avance III 400 with an automatic tuning and matching multinuclear gradient probe. Spectra were acquired at 27, 60, and 120 °C, with 600 s equilibration time. In all cases, standard 5 mm borosilicate NMR tubes were used.

Differential scanning calorimetry (DSC). Thermal profiles of the nanoparticle formation were obtained using a TA DSC Q2000 model with a TA Refrigerated Cooling System 90 (RCS), with the reaction mixture sealed in TA Tzero alodined pans with hermetic alodined lids. The temperature was ramped from 25 to 150 °C, at 2 °C min^{-1} rate, with a cooling rate of 10 °C min^{-1}, in two cycles. Glass transition temperatures were measured using a TA DSC Q2000 model with a TA Liquid Nitrogen Cooling System (LNCS). The samples were sealed in the glovebox, in TA Tzero aluminium pans with aluminium hermetic lids. A cooling and heating ramp of 5 °C min^{-1} was used, within the temperature ranging from –150 to 100 °C, and three scans were carried out for each sample.

Thermogravimetric analysis (TGA). The temperature of decomposition was measured using a TA TGA Q5000, at a heating rate of 5 °C min^{-1}. All samples were sealed in the glovebox, in aluminium pans. The onset of the weight loss in each thermogram was used as a measure of the decomposition temperature.

Karl Fischer analysis. The water content of ionic liquids was measured by coulometric Karl Fischer titration using a GRScientific Cou-Lo Aquamax KF Moisture Meter. All samples were dried under high vacuum (60 °C, overnight) and stored in the glovebox prior to the measurements.

Transmission electron microscopy (TEM). TEM images were acquired in bright field using a Tecnai 200 kV F20 Transmission Electron Microscope with a Field Emission Gun. A few drops of sample were pipetted onto an Agar holey carbon film copper TEM grids and inserted into the microscope. In the case of the phosphonium-based IL-nanofluids, the samples were diluted with acetone, and the prepared grid was set aside for *ca.* 20 min prior to inserting it into the microscope, in order to allow the solvent to evaporate. Images were taken with a Gatan CCD digital camera attached to the microscope.

X-Ray Photoelectron Spectroscopy (XPS). The XPS spectra were obtained using a Kratos AXIS Ultra DLD XPS spectrometer using monochromated Al Kα X-rays and a hemispherical analyser with a pass energy of 160 eV. The IL-nanofluid samples were mounted on conducting copper tape and the binding energies were normalised to the C 1 s at 284.6 eV. Background subtraction was performed using a Shirley background and CasaXPS.[42]

Density. Density was measured using a Mettler Toledo DE40 density meter, within 25–85 °C, in 10 °C increments. Tested samples were loaded into syringes in the glovebox and transferred immediately to the apparatus.

Crystallography. The single-crystal X-ray structure determination was carried out at 100 K using an Oxford Diffraction Gemini diffractometer. The images were interpreted and integrated with CrysAlisPro.[43] The structure was solved by direct methods and refined by full-matrix least-squares on F^2 using OLEX^2 and the SHELX program package.[44] Non-hydrogen atoms were anisotropically refined and the hydrogen atoms were refined in the riding mode with isotropic temperature factors fixed at 1.2 times U(eq) of the parent atoms (1.5 times for methyl groups). CCDC 839595 contains the supplementary

crystallographic data for this paper and it can be obtained free of charge *via* www.ccdc.cam.ac.uk/conts/retrieving.html (or from the Cambridge Crystallographic Data Centre, 12, Union Road, Cambridge CB2 1EZ, UK; fax: +44-1223-336033; or deposit@ccdc.cam.ac.uk).†

Results and discussion

Choice of ionic liquids and reaction conditions

The use of task-specific ionic liquids incorporating a basic acetate anion, acting as a base and a stabilising agent, allowed for the facile, one-pot preparation of stable nanoparticle dispersions in ionic liquids (IL-nanofluids), in an extremely material-efficient process. The two cations chosen were of a very different nature: $[C_4mim]^+$ is hydrophilic, aromatic and known to be able to coordinate as a carbene to metals, whereas $[P_{8\,8\,8\,12}]^+$ is hydrophobic, aliphatic and non-coordinating. This selection allowed us to examine the influence of the cation on the formation of copper oxide nanostructures.

The synthesis was initially investigated by carrying out the reactions in sealed DSC pans. Stock solutions of copper(II) acetate hydrate in $[P_{8\,8\,8\,12}][OAc]$ and in $[C_4mim][OAc]$ were heated slowly (2 °C min^{-1}) to 150 °C, then cooled rapidly to room temperature and the cycle was repeated. As shown in Fig. 1, for both solutions, exothermic reactions (negative peaks) took place only in the first cycles. The reactions were not reversible, and completed within the time of the first cycle and, therefore, in second cycles the heat flow *vs.* temperature remained linear, *i.e.* no exothermic effect was observed.

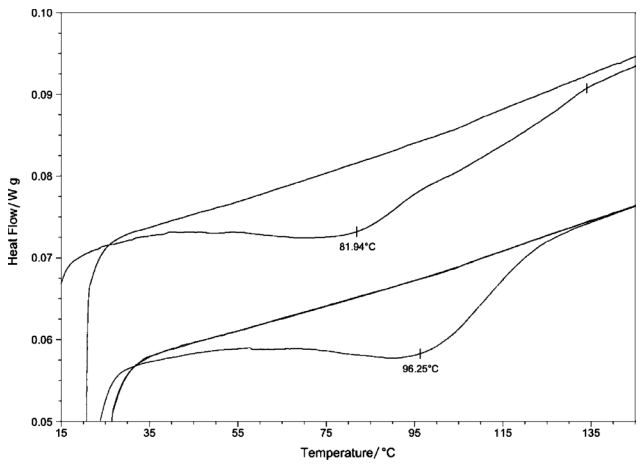

Fig. 1 Thermal profiles of the DSC-monitored formation of IL-nanofluids based on $[P_{8\,8\,8\,12}][OAc]$ (top) and $[C_4mim][OAc]$ (bottom). In both cases, first heating cycles show exothermic (negative) processes that are not reproduced in the second and subsequent heating cycles, indicating complete and irreversible reactions.

Based on the DSC tests, a temperature of 120 °C was chosen for further reactions. This temperature enabled fast reaction rates, and at the same time prevented thermal decomposition of the acetate-based ionic liquids (for thermal properties of the used ionic liquids see Table 2).

Ultrasound treatment of the reaction mixture is known to decrease the size of the formed nanoparticles and reduce aggregation. Therefore, for each ionic liquid system, two modes of agitation were tested: stirring using a conventional magnetic stirring bar, and ultrasound agitation with a sonic probe.

Characterisation of formed CuO and Cu_2O particles

X-Ray Photoelectron Spectroscopy (XPS). All IL-nanofluids were analysed using XPS and the binding energies were normalised to the C 1s at 284.6 eV; the spectra obtained are shown in Fig. 2.

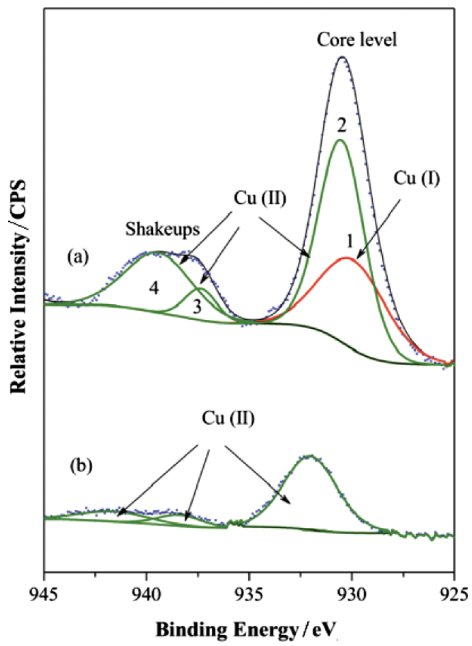

Fig. 2 XPS spectra for Cu $2p_{3/2}$ spectral lines of nanoparticles synthesised using magnetic stirring in: (a) $[C_4mim][OAc]$ and (b) $[P_{8\,8\,8\,12}][OAc]$. Peak 1 represents copper(I) and peaks 2–4 represent copper(II).

Fig. 2a shows the peak fit of Cu $2p_{3/2}$ core level and its corresponding shake-up satellites for the sample based on $[C_4mim][OAc]$. The dotted blue line represents the original data; peak fits of the individual components are shown using coloured solid lines, while their sum is shown as the black solid line. Cu $2p_{3/2}$ peak 1, positioned at the binding energy value of 932.5 eV (red line) is assigned to the Cu(I) state and peak 2 positioned at 933.1 eV (green line) is assigned to Cu(II) state.[45] The additional peaks (3 and 4) around 940 eV in the Cu $2p_{3/2}$ peak region result from a shake up process due to the open $3d^9$ shell of Cu(II). The relative amount of Cu(II) to Cu(I) state present on the surface was $[Cu^{2+}]/[Cu^{+}] = 2.4$, obtained from the ratio of the sum of the areas of peaks 2–4 to that of peak 1.[46]

For the sample based on $[P_{8\,8\,8\,12}][OAc]$— Fig. 2b —the Cu $2p_{3/2}$ peak is positioned at the binding energy value 932.6 eV (green line) along with shake-up satellites around 940 eV indicating Cu(II) state.

XPS analysis strongly indicate, that a mixed valent copper(I,II) oxide has formed in $[C_4mim][OAc]$, while copper(II) oxide has been synthesised in $[P_{8\,8\,8\,12}][OAc]$. Regarding other possible copper-containing species, it has already been demonstrated by the DSC experiment (Fig. 1), that no residual copper(II) acetate has been left after the synthesis. In the XPS experiments, no evidence for the presence of copper hydroxide, copper acetate or a copper carbene

complex was found, as the binding energy for the Cu $2p_{3/2}$ peak from copper acetate species would be seen at *ca.* 934.0 eV; copper hydroxide 934.5–935.0 eV, while that of a copper carbene complex species would be seen at *ca.* 936.0 eV.[47]

Transmission Electron Microscopy (TEM). TEM images of synthesised copper oxide nanostructures are presented in Fig. 3. All images were taken directly in ionic liquid.

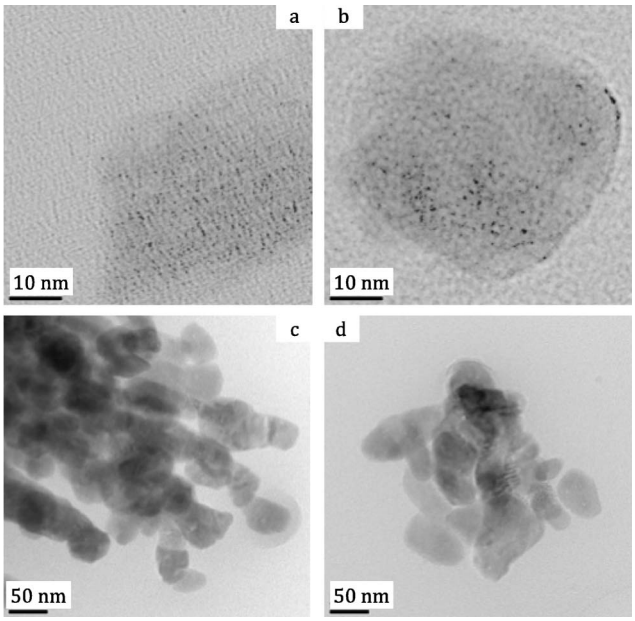

Fig. 3 TEM images of copper(I,II) oxide clusters and copper(II) oxide nanoparticles synthesised in [C_4mim][OAc], using magnetic stirring (a) and ultrasound (b), and in [$P_{8\,8\,8\,12}$][OAc], using magnetic stirring (c) and ultrasound (d).

Fig. 3a and b show small droplets of [C_4mim][OAc] with barely-visible mixed-oxidation state clusters of copper(I,II) oxide. Nanoparticles of copper(II) oxide prepared in [$P_{8\,8\,8\,12}$][OAc] were much larger, with diameters of *ca.* 50 nm, as shown in Fig. 3c and d. Surprisingly, the use of ultrasound did not have observable influence on the decrease of the nanoparticles size. This may indicate a very rapid formation of the particles, with no time for the cavitation bubbles to affect the process.

Study of formation of copper(I,II) oxide clusters and copper(II) oxide nanoparticles

It has been found, that a simple variation of a cation has a tremendous influence on the chemistry of the process and, as a result, on the morphology of the formed species. It appeared important to study the differences in both formation mechanisms, and the role of the cation in particular.

DSC scans. As shown in Fig. 1, DSC scans related to the reactions in both ionic liquids have different thermal profiles. The peak corresponding to an exothermic reaction in [C_4mim][OAc] was symmetrical, with maximum at *ca.* 96 °C. In contrast, the maximum exotherm for the [$P_{8\,8\,8\,12}$][OAc]-based solution was much lower (*ca.* 82 °C), but the DSC scan featured a shoulder, extending to nearly 135 °C. This may indicate two steps in the formation of copper(II) oxide nanoparticles.

UV-VIS spectroscopy. It has been found, that upon rapid heating (*ca.* 20 °C min^{-1}), the colour of the reaction mixtures changed several times, the changes depending strongly on the ionic liquid cation.

At room temperature, a solution of copper(II) acetate hydrate in [$P_{8\,8\,8\,12}$][OAc] was blue, with the typical absorption band of a hydrated copper(II) acetate species at 370 nm and 690 nm.[48] Upon heating to about 60 °C, the colour changed to green (absorption bands at 370 nm, 420 nm and 700 nm), indicating a transition to a partly dehydrated, or possibly hydroxygenated, copper(II) species. Further heating of the solution to about 120 °C resulted in the formation of a dark brown liquid, with an absorption maximum at 850 nm, which suggests the formation of copper(II) oxide.

The solution of the copper(II) acetate hydrate in [C_4mim][OAc] was also blue at room temperature (broad absorption band at 630 nm, see Fig. 4, curve 1).

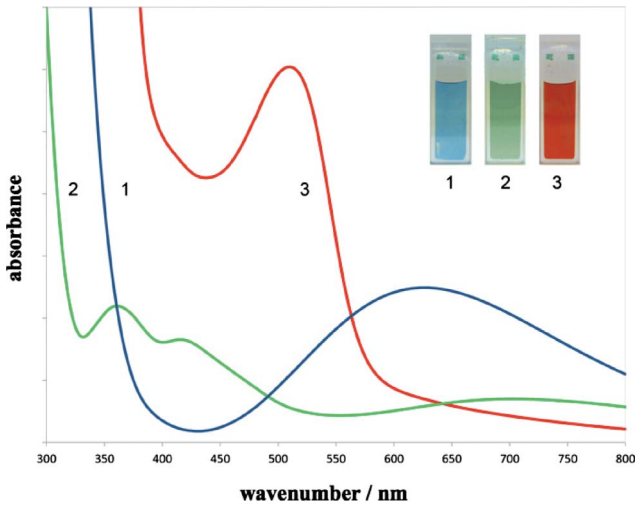

Fig. 4 Colour changes observed during the synthesis of Cu_2O clusters in [C_4mim][OAc], illustrated by photographs and corresponding UV-VIS spectra.

Upon careful heating to about 70 °C, the solution turned green, with a broad band at about 700 nm (Fig. 4, curve 2). Further heating to 120 °C resulted in a deep red liquid, very different in appearance from the product obtained in [$P_{8\,8\,8\,12}$][OAc]. The UV-VIS spectrum exhibited an absorption maximum at 530 nm (Fig. 4, curve 3), indicating the formation of a colloid.

The UV-VIS studies indicate, that both processes go through a similar first step, involving a partial dehydration of the solution copper(II) species. For [$P_{8\,8\,8\,12}$][OAc], the second step appears to involve thermal decomposition of the coordination of the solution species (in accordance with the shoulder on the DSC scan, Fig. 1). At the same time, the second step in [C_4mim][OAc] must include decomposition of the solution species, along with a partial reduction of the copper(II) to copper(I). The partially dehydrated intermediate species (green solution) appeared to be unstable, and the green colour was only observed for a few minutes, after very slow and careful heating, with quick subsequent transformation to the final product. Therefore, the formation of the partially dehydrated species is most likely the rate-limiting step, followed by a rapid decomposition. This is in agreement with a single peak found in the DSC scan (Fig. 1).

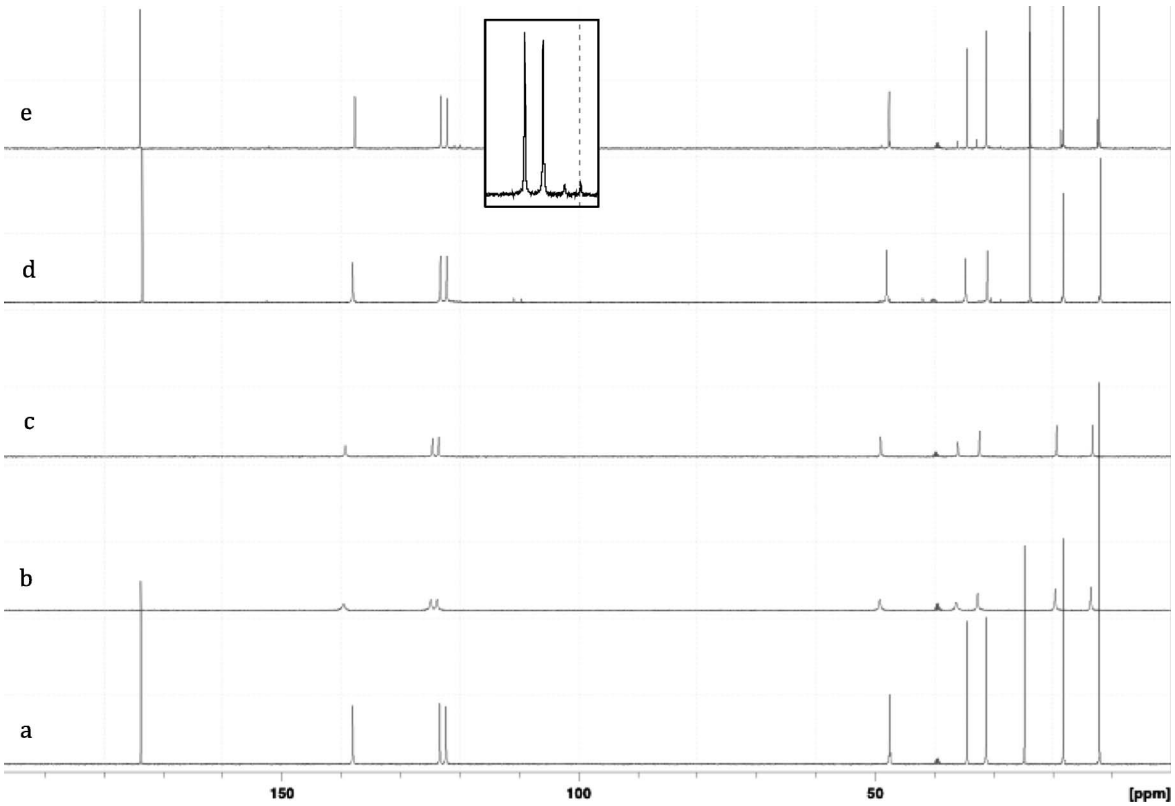

Fig. 5 ^{13}C NMR spectra (100.6 MHz, neat liquid, DSMO as reference) of [C_4mim][OAc] at 27 °C (a), as well as a copper(II) acetate hydrate solution in [C_4mim][OAc], at: 27 °C (b), 60 °C (c), 120 °C (d), and subsequently cooled down to 27 °C (e). The insert shows the magnified part of the spectrum (e), with the carbene signals clearly visible.

^{13}C NMR spectroscopy. Further studies of the nanoparticle formation were carried out using variable temperature ^{13}C NMR spectroscopy. Neat starting solutions (blue) were placed in NMR tubes, and the ^{13}C NMR spectra were acquired firstly at ambient temperature (27 °C), then at 60 °C (the temperature at which the solution changed the colour to green in the case of the [$P_{8\,8\,8\,12}$][OAc] system), at 120 °C, and finally again at 27 °C. These results were compared to the ambient temperature ^{13}C NMR spectra of the corresponding neat ionic liquids. The ^{13}C NMR spectra for the [C_4mim][OAc]-based system are compared in Fig. 5.

^{13}C NMR spectrum of neat [C_4mim][OAc] shows the pure ionic liquid (Fig. 5a), with the ^{13}C NMR signal from the (C═O) carbon at δ = 174 ppm. This signal is not observed in the spectra of the copper(II) acetate hydrate solution in [C_4mim][OAc] at 27 °C (blue) and 60 °C (green), because all acetate anions in solution are in a dynamic equilibrium with those complexed to the paramagnetic copper(II). Upon further heating, the solution species of copper(II) decompose to yield copper(I,II) oxide (red colloid), and the acetate anions are no longer coordinating to copper. Therefore, at 120 °C the acetate signal is visible again (Fig. 5d); it is also visible in the ambient temperature spectrum of the prepared IL-nanofluid (Fig. 5e), showing that an irreversible reaction took place. The analogous observations regarding the signal from the (C═O) carbon were made for the acetate signals in the ^{13}C NMR spectra of the [$P_{8\,8\,8\,12}$][OAc]-based mixtures.

Regarding the ^{13}C NMR signals from the cations of the respective ionic liquids, it was found that the [$P_{8\,8\,8\,12}$]$^+$ cation remained unaffected throughout the reaction, whereas for the IL-nanofluid based on [C_4mim][OAc], a new set of low-intensity signals appeared after the reaction (see Fig. 5d, e, and the insert). This set of peaks, corresponding to a new species based on the 1-butyl-3-methylimidazolium cation, was firstly observed at 120 °C (*i.e.* after the final step of the reaction), and subsequently also in the spectrum of the IL-nanofluid at 27 °C. The peaks of the imidazolium ring are shifted upfield, which indicates increased electron density on the ring, and thereby a possible carbene formation, which has been reported earlier to easily occur for imidazolium salts in the presence of copper(II) under basic conditions.[49]

Crystallisation of a structure from precursor solution. In order to elucidate the intermediate species in the course of the nanoparticle formation, particularly in the imidazolium-based system, it has been attempted to crystallise a precursor complex from the solution. However, since crystallisation from [C_4mim][OAc] was unsuccessful, an ionic liquid with a shorter alkyl chain on the cation (and therefore more prone to provide crystalline species), namely 1-ethyl-3-methylimidazolium acetate, [C_2mim][OAc], was examined.

Upon heating the highly concentrated (1.8 M) solution of copper(II)acetate hydrate in [C_2mim][OAc] to about 70 °C, the solution colour changed gradually from blue to green. Subsequent slow cooling to room temperature resulted in the crystallisation of small, transparent, green crystals. Single crystal X-ray structure determination of this crystalline precipitate revealed the structure of the compound [C_2mim][$Cu_3(OAc)_5(H_2O)(OH)_2$]·H_2O

Table 1 Crystal data for $[C_2mim][Cu_3(OAc)_5(H_2O)(OH)_2]\cdot H_2O$

Empirical formula	$C_{32}H_{60}Cu_6N_4O_{28}$
Formula weight	1330.08
T/K	100(2)
Wavelength	Mo-Kα0.71073
Crystal system	Monoclinic
Space group	Cc
a/Å	10.5009(3)
b/Å	21.7757(6)
c/Å	10.8067(3)
α (°)	90.00
β (°)	93.286(3)
γ (°)	90.00
volume/Å^{-3}	2467.05(12)
Z	2
D_c (mg m^{-3})	1.791
Absorption coefficient μ/mm^{-1}	2.633
F(000); no. of parameters	1356; 349
Crystal size/mm	0.20 × 0.20 × 0.20
θ range (°)	5.88, 52.74
Flack parameter	0.085(17)
Index ranges	$-12\leq h\leq 13$, $-27\leq k\leq 27$, $-13\leq l\leq 12$
Independent reflections, R_{int}	4284, R_{int} = 0.0487
Goodness-of-fit (F^2)	1.054
Final R indices $I > 2\sigma(I)$	R = 0.0373, wR = 0.0900
R indices (all data)	R = 0.0454, wR = 0.0947
R_{int}	R_{int} = 0.0487

(see Table 1). This structure consists of $[C_2mim]^+$ cations and an anionic copper oxy-hydroxy strand (Fig. 6a), consisting of triangles of copper atoms bridged by μ_3-OH. Each of those Cu triangles is connected to two adjacent μ_3-OH bridged Cu triangles, *via* an edge on the one side and *via* the corner on the other (Fig. 6b). The three crystallographically independent copper atoms are also connected by acetate anions in bridging and chelating-bridging mode, as illustrated in Fig. 6c—leading to an approximately hexagonal Cu_3O_3 motif. The coordination spheres of the three copper atoms can roughly be described as CuO_6 octahedra, however with a Jahn–Teller distortion with Cu–O distances ranging for Cu1 from 1.948 to 2.522 Å; for Cu2 from 1.944 to 2.788 Å, and for Cu3 from 1.946 to 2.557 Å. The copper–copper distances are rather short, with Cu1–Cu2 = 3.172(10) Å, Cu2–Cu3 = 3.0022(9) Å and Cu3–Cu1 = 3.166(10) Å.

The coordinating water molecules were hydrogen bonding to the acetate anions, with O–H···O distances ranging from 1.735 Å to 1.815 Å. Further hydrogen bonding was found for the acidic hydrogen of the imidazolium cation to one of the oxygen atoms of a coordinating acetate anion, with an O–H···O distance of 2.245(4) Å. In the packing of the structure the distance of the copper strands (measured for the shortest distance of the centroids of the copper triangles of adjacent strands) is about 10.5 Å.

Only a few copper(II) hydroxy salts with the hexagonal Cu_3O_3 motif have been reported to date, most of them related to the solid state structure of compounds such as the mineral botallackite, $Cu_2(OH)_3Cl$, or the compound $Cu_2(OH)_3(NO_3)$, which are all based on $Cu_2(OH)_3X$ layers of hexagonally packed copper atoms. Furthermore, the crystal structure of a basic copper(II) acetate, $Cu_2(OH)_3(CH_3COO)\cdot H_2O$, reported by Masciocchi *et al.*,[50] had a similar sheet structure. Apparently, in the presence of the $[C_2mim]^+$ cation, the formation of an anionic strand in $[C_2mim][Cu_3(OAc)_5(H_2O)(OH)_2]\cdot H_2O$ is favoured. The ionic nature of this compound is probably facilitating its crystallisation, in contrast to the mentioned basic copper(II) acetate that precipitates as a microcrystalline powder.[50]

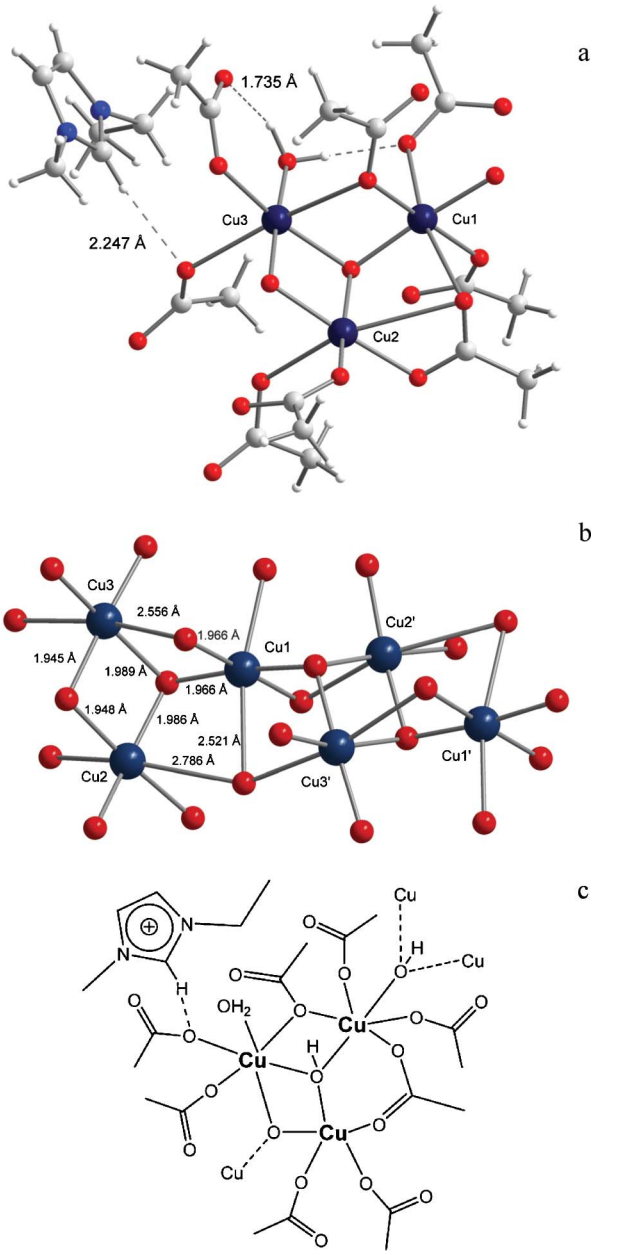

Fig. 6 Crystal structure of $[C_2mim][Cu_3(OAc)_5(H_2O)(OH)_2]\cdot H_2O$: (a) cationic and anionic strand; (b) connectivity and distances along the copper strands; (c) schematic drawing of the structure.

Suggested formation mechanism of copper(II) oxide nanoparticles and mixed valent copper oxide clusters. The formation of CuO nanoparticles from a solution of copper(II) acetate hydrate in $[P_{8\,8\,8\,12}][OAc]$ can be attributed to the initial formation of anionic basic species (blue solution), subsequently dehydrated or partially dehydrated (green solution) and then undergoing thermal decomposition to yield copper(II) oxide (brown IL-nanofluid, containing nanoparticles of *ca.* 50 nm). This is in agreement with previous reports on the decomposition/dehydration reactions of copper(II) salts in the course of the CuO formation after addition of a base (hydroxides).[51]

Table 2 Values of glass transition temperatures, decomposition temperatures and water content of pure ionic liquids, [C_4mim][OAc] and [$P_{8\,8\,8\,12}$][OAc], and the derived IL-nanofluids, prepared using either magnetic stirring (st) or ultrasound (us)

	glass transition/°C			
system	glass → liquid	liquid → glass	T_d/°C	H_2O content/wt %
[C_4mim][OAc]	60.18	60.11	208.71	0.0978
[C_4mim][OAc]-Cu_xO (st)	63.01	62.18	200.03	0.0102
[C_4mim][OAc]-Cu_xO (us)	63.90	66.28	199.86	0.0119
[$P_{8\,8\,8\,12}$][OAc]	75.74	74.32	274.74	0.0248
[$P_{8\,8\,8\,12}$][OAc] - CuO (st)	80.09	79.14	272.68	0.2536
[$P_{8\,8\,8\,12}$][OAc] - CuO (us)	79.64	81.31	268.16	0.2249

The postulated reaction mechanism follows eqn (1), starting from the binuclear copper(II) acetate.

$$Cu_2(OAc)_4{\cdot}2H_2O + 2\,[P_{8\,8\,8\,12}][OAc] \rightarrow [P_{8\,8\,8\,12}]_2[Cu_2(OAc)_4(OH)_2] + 2\,HOAc \rightarrow 2\,CuO + 2\,[P_{8\,8\,8\,12}][OAc] + 4\,HOAc \quad (1)$$

In the course of the reaction, the acetate anions in the ionic liquid remain in a dynamic equilibrium with those coordinating to copper atoms, and are thus invisible on the ^{13}C NMR spectra (see Fig. 5b and c). After the reaction, the solubilised acetic acid is dissociated in ionic liquid, and all the acetate groups are equal by ^{13}C NMR spectroscopy (Fig. 5d and e). The ionic liquid here has multiple roles of the base (acetate) donor, stabiliser of the proposed ionic intermediate, $[Cu_2(OAc)_4(OH)_2]^{2-}$, and stabiliser of the nanoparticles in the formed IL-nanofluid.

The first stage of the formation of copper(I,II) oxide clusters in [C_4mim][OAc] resembles the formation of copper(II) oxide. As shown in Fig. 4, upon heating, the solution of hydrated copper species (blue) is partially dehydrated (green), and forms copper oxo-hydroxy species. This was supported by UV-VIS spectroscopy, and by the crystallisation of the compound $[C_2mim][Cu_3(OAc)_5(H_2O)(OH)_2]{\cdot}H_2O$ from its analogue, green [C_2mim][OAc]-based precursor solution (Fig. 6). Of course, it is worth noting, that the solution species cannot be identical with this polymeric structure, and the solid-state structures may be merely indications for the structure of the solution species.[52] This rate-limiting step was followed by decomposition of the complex, combined with a reduction of copper(II) to copper(I), to yield the red IL-nanofluid containing Cu_2O clusters.

Since this second step only took place in the imidazolium-based ionic liquid, and not in the phosphonium-based one, it can be concluded that the $[C_4mim]^+$ cation is actively involved in the reduction process. Considering the basicity of the acetate solutions and the acidity of the proton on the imidazolium ring, this step may involve the removal of acetic acid from the complex presented in Fig. 6c, and formation of a 1,3-dialkylimidazolium carbene. A similar mechanism has been found for several other transition metals in the presence of imidazolium and a base.[53] It may be postulated, that decomposition of such a carbene complex could result in the partial reduction of copper(II) to copper(I), which is supported by the presence of carbene signals in the ^{13}C NMR spectra after the reaction (Fig. 5d and e).

Table 3 Experimental values of density, ρ/g cm^{-3}, measured for the pure ionic liquids and the corresponding IL-nanofluids, prepared using either magnetic stirring (st) or ultrasound (us)

	ρ/g cm^{-3}		
T/°C	[C_4mim][OAc]	+ Cu_xO (st)	+ Cu_xO (us)
25	1.0651	1.0670	1.0667
35	1.0588	1.0603	1.0603
45	1.0526	1.0538	1.0539
55	1.0465	1.0475	1.0476
65	1.0406	1.0414	1.0414
75	1.0346	1.0353	1.0352
85	1.0288	1.0292	1.0291
	[$P_{8\,8\,8\,12}$][OAc]	+ CuO (st)	+ CuO (us)
25	0.8897	0.9118	0.9076
35	0.8836	0.9054	0.9014
45	0.8775	0.8991	0.8952
55	0.8714	0.8927	0.8889
65	0.8653	0.8862	0.8827
75	0.8593	0.8797	0.8764
85	0.8533	0.8733	0.8703

Physical properties of the prepared IL-nanofluids

Temperatures of glass transition and decomposition. Thermal properties of neat ionic liquids and prepared IL-nanofluids, as well as the water content of the tested samples, are shown in Table 2.

Presence of the copper oxide nanostructures affected slightly both glass transition temperatures and decomposition temperatures. However, this effect is too small to have any practical significance. The materials incorporating the imidazolium-based anions have lower decomposition temperatures, as the acetate anion can easily remove the acidic proton from the imidazolium ring.

Density. Densities of neat ionic liquids and corresponding IL-nanofluids were measured in a range of temperatures (see Table 3 and Fig. 7).

Interestingly, densities of the IL-nanofluids based on [C_4mim][OAc] were almost identical with the neat ionic liquid, despite the addition of copper(II) acetate–probably due to the small size of the clusters.

Densities of the IL-nanofluids based on [$P_{8\,8\,8\,12}$][OAc] were, as expected, higher than the density of the neat ionic liquid. This may be explained by the presence of relatively large (*ca.* 50 nm) nanoparticles of copper(II) oxide, of a density obviously higher than the ionic liquid itself. Furthermore, density of the IL-nanofluid produced using ultrasound was found to be slightly higher than the density of the IL-nanofluid synthesised using magnetic stirring. This may suggest that the ultrasound

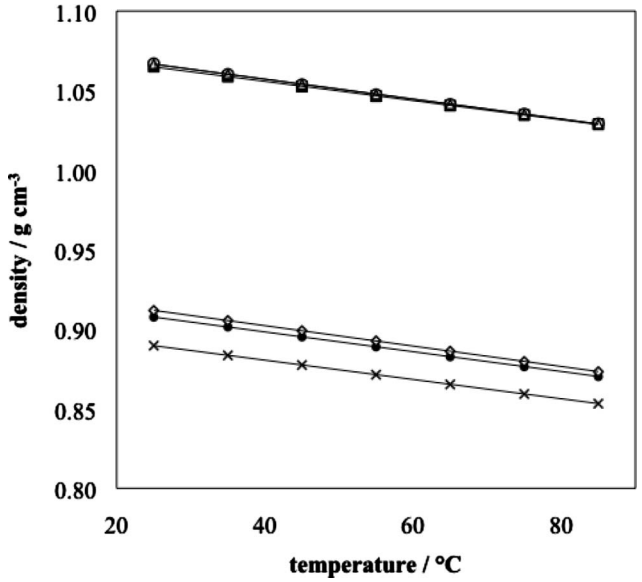

Fig. 7 Experimental densities as a function of temperature, plotted for $[P_{8\,8\,8\,12}][OAc]$, ×, two IL-nanofluids prepared based on this ionic liquid using magnetic stirring, ●, and ultrasound, ◇, as well as for pure $[C_4mim][OAc]$, ■, and two IL-nanofluids prepared based on this ionic liquid using magnetic stirring, ○, and ultrasound, ▲.

Table 4 Correlation parameters of the density *vs.* temperature plot for two neat ionic liquids, $[C_4mim][OAc]$ and $[P_{8\,8\,8\,12}][OAc]$, and derived IL-nanofluids, prepared using either magnetic stirring (st) or ultrasound (us)

system	*a*	*b*	R^2
$[C_4mim][OAc]$	–0.00060	1.07997	0.99982
$[C_4mim][OAc]$-CuO st	–0.00063	1.08232	0.99966
$[C_4mim][OAc]$-CuO us	–0.00063	1.08222	0.99992
$[P_{88812}][OAc]$	–0.00061	0.90485	0.99999
$[P_{88812}][OAc]$-CuO st	–0.00064	0.92792	0.99999
$[P_{88812}][OAc]$-CuO us	–0.00062	0.92321	0.99999

treatment had some effect on the morphology and/or size of the nanoparticles, albeit it was too subtle to be observable by TEM.

The experimental densities, ρ/g cm^{-3}, were correlated with temperature, T/°C using a linear regression, according to eqn (2).

$$\rho = aT + b \quad (2)$$

The correlation parameters for are shown in Table 4.

Stability of the nanofluids

All prepared IL-nanofluids remained stable, even over the course of several months; no precipitation was observed after this time. Moreover, it was not possible to separate the suspension by intensive centrifugation (2000 rpm, 3 h).

IL-nanofluids based on $[P_{8\,8\,8\,12}][OAc]$ seemed to be unaffected by atmospheric conditions, while those incorporating $[C_4mim][OAc]$ changed colour to green after prolonged (overnight) exposure to the open air, which indicates the reoxidation of Cu(I) to Cu(II).

Conclusions

We report a facile method for the *in situ* synthesis of stable copper(II) oxide nanoparticles and copper(I,II) oxide clusters in acetate-based ionic liquids. Depending on the cation of the ionic liquid, the synthetic method produces CuO nanoparticles of a mean diameter below 50 nm in $[P_{8\,8\,8\,12}][OAc]$, or Cu_xO (I,II) clusters in $[C_4mim][OAc]$. These ionic liquid-based nanofluids can be prepared with a high loading of copper oxide, and do not precipitate for at least several months. The combination of DSC experiments, UV-VIS spectroscopy, variable temperature ^{13}C NMR spectroscopy and crystallography revealed different formation mechanisms, with both anions and cations of the ionic liquids playing a significant role. The physical properties of the IL-nanofluids were characterised, revealing an influence of the particle size on the density of the IL-nanofluids. The nanocomposite materials produced have a great potential for the use as catalysts or heat transfer fluids.

Acknowledgements

Al Robertson (Cytec) is acknowledged for the supply of trioctylphosphine and Stephen MacFarland for invaluable experimental assistance with TEM measurements. The authors acknowledge QUILL and its Industrial Advisory Board, as well as the EPSRC (Portfolio Partnership Grant EP/D029538/1), for support. P.N. thanks the EPSRC for a RCUK fellowship. The EPSRC UK National Crystallography Service (NCS) and Marcus Winter and Oliver Presly from Agilent (Oxford Diffraction) are acknowledged for crystal data collection.

Notes and references

1 S. U. S. Choi, Enhancing thermal conductivity of fluids with nanoparticles, in: D. A. Singer, H. P. Wang (ed.), *Developments and Applications of Non-Newtonian Flows*, vol. 231, ASME, New York, 1995, pp. 99.
2 C. Guerrero-Sanchez, T. Lara-Ceniceros, E. Jimenez-Regalado, M. Raşa and U. S. Schubert, *Adv. Mater.*, 2007, **19**, 1740.
3 E. Andablo-Reyes, R. Hidalgo-Alvarez and J. de Vicente, *Soft Matter*, 2011, **7**, 880.
4 M. Baglioni, D. Rengstl, D. Berti, M. Bonini, R. Giorgi and P. Baglioni, *Nanoscale*, 2010, **2**, 1723.
5 K. Lunstroot, L. Baeten, P. Nockemann, J. Martens, P. Verlooy, X. P. Ye, C. Görller-Walrand, K. Binnemans and K. Driesen, *J. Phys. Chem. C*, 2009, **113**, 13532.
6 A. Caballero, J. Morales, L. Sanchez and Electrochem, *Electrochem. Solid-State Lett.*, 2005, **8**, A464.
7 P. Wang, S. M. Zakeeruddin, J.-E. Moser and M. Grätzel, *J. Phys. Chem. B*, 2003, **107**, 13280.
8 for example: (*a*) J. Dupont, G. S. Fonseca, A. P. Umpierre, P. F. P. Fichtner and S. R. Teixeira, *J. Am. Chem. Soc.*, 2002, **124**, 4228; (*b*) E. Redel, J. Krämer, R. Thomann and C. Janiak, *J. Organomet. Chem.*, 2009, **694**, 1069; (*c*) C. Vollmer, E. Redel, K. A. -Shandi, R. Thomann, H. Manyar, C. Hardacre and C. Janiak, *Chem.–Eur. J.*, 2010, **16**, 3849.
9 *Ionic Liquids in Synthesis*, ed. P. Wasserscheid and T. Welton, Willey Interscience, Weinheim, 2nd ed., 2007.
10 N. Plechkova and K. R. Seddon, *Chem. Soc. Rev.*, 2008, **37**, 123.
11 M. Freemantle, *Chem. Eng. News*, 1998, **76**, 32.
12 For example: (*a*) F. Endres, *ChemPhysChem*, 2002, **3**, 144; (*b*) M. Armand, F. Endres, D. R. MacFarlane, H. Ohno and B. Scrosati, *Nat. Mater.*, 2009, **8**, 621.
13 (*a*) V. I. Pârvulescu and C. Hardacre, *Chem. Rev.*, 2007, **107**, 2615; (*b*) M. J. Muldoon, *Dalton Trans.*, 2010, **39**, 337; (*c*) H. Olivier-Bourbigou, L. Magna and D. Morvan, *Appl. Catal., A*, 2010, **373**, 1; (*d*) J. P. Hallett and T. Welton, *Chem. Rev.*, 2011, **111**, 3508.

14 For example: (*a*) M. E. Van Valkenburg, R. L. Vaughn, M. Williams, and A. J. S. Wilkes, presented at Fifteenth Symposium on Thermophysical Properties, June 22, 2003, Boulder, Colorado, USA; (*b*) J. D. Holbrey, *Chim Oggi*, 2007, **25**, 24; (*c*) 1. Y. U. Paulechka, A. G. Kabo, A. V. Blokhin, G. J. Kabo and M. P. Shevelyova, *J. Chem. Eng. Data*, 2010, **55**, 2719.

15 For example: (*a*) F. Zhou, Y. Liang and W. Liu, *Chem. Soc. Rev.*, 2009, **38**, 2590; (*b*) T. Predel, B. Pohrer and E. Schlücker, *Chem. Eng. Technol.*, 2010, **33**, 132–136.

16 K. Lunstroot, K. Driesen, P. Nockemann, C. Gorller-Walrand, K. Binnemans, S. Bellayer, J. Le Bideau and A. Vioux, *Chem. Mater.*, 2006, **18**, 5711; K. Lunstroot, K. Driesen, P. Nockemann, K. Van Hecke, L. Van Meervelt, C. Gorller-Walrand, K. Binnemans, S. Bellayer, L. Viau, J. Le Bideau and A. Vioux, *Dalton Trans.*, 2009, 298.

17 A. Noda and M. Watanabe, *Electrochim. Acta*, 2000, **45**, 1265.

18 T. Fukushima, A. Kosaka, Y. Ishimura, T. Yamamoto, T. Takigawa, N. Ishii and T. Aida, *Science*, 2003, **300**, 2072.

19 for example: (*a*) A. Taubert, *Acta Chim. Slov.*, 2005, **52**, 183; (*b*) J. B. Willems, H. W. Rohm, C. Geers and M. Köckerling, *Inorg. Chem.*, 2007, **46**, 6197.

20 (*a*) D. Nakamura, I. Gunjishima, S. Yamaguchi, T. Ito, A. Okamoto, H. Kondo, S. Onda and K. Takatori, *Nature*, 2004, **430**, 1009; (*b*) E. R. Parnham, P. S. Wheatley and R. E. Morris, *Chem. Commun.*, 2006, 380.

21 (*a*) Y. Zhou and M. Antonietti, *Adv. Mater.*, 2003, **15**, 1452; (*b*) A. Taubert, *Angew. Chem., Int. Ed.*, 2004, **43**, 5380; (*c*) A. V. Mudring, T. Alammar, T. Backer and K. Richter, in Ionic Liquids: From Knowledge to Application, ed. N. V. Plechkova, R. D. Rogers, K. R. Seddon, *ACS Symposium Series*, 2009, **1030**, 177; (*d*) N. P. Tarasova, Y. V. Smetannikov and A. A. Zanin, *Russ. Chem. Rev.*, 2010, **79**, 463.

22 N. R. Rao, G. U. Kulkarni, P. J. Thomas and P. P. Edwards, *Chem. Soc. Rev.*, 2000, **29**, 27.

23 (*a*) P. Nockemann, M. Pellens, K. Van Hecke, L. Van Meervelt, J. Wouters, B. Thijs, E. Vanecht, T. N. Parac-Vogt, H. Mehdi, S. Schaltin, J. Fransaer, S. Zahn, B. Kirchner and K. Binnemans, *Chem.–Eur. J.*, 2010, **16**, 1849; (*b*) P. Nockemann, B. Thijs, T. N. Parac-Vogt, K. Van Hecke, L. Van Meervelt, B. Tinant, I. Hartenbach, T. Schleid, V. T. Ngan, M. T. Nguyen and K. Binnemans, *Inorg. Chem.*, 2008, **47**, 9987.

24 For example: (*a*) J. B. Rollins, B. D. Fitchett and J. C. Conboy, *J. Phys. Chem. B*, 2007, **111**, 4990; (*b*) T. Gutel, J. Garcia-Antõn, K. Pelzer, K. Philippot, C. C. Santini, Y. Chauvin, B. Chaudret and J. Basset, *J. Mater. Chem.*, 2007, **17**, 3290.

25 For example: (*a*) L. S. Ott, M. L. Cline, M. Deetlefs, K. R. Seddon and R. G. Finke, *J. Am. Chem. Soc.*, 2005, **127**, 5758–5759; (*b*) K. Ueno, A. Inaba, M. Kondoh and M. Watanabe, *Langmuir*, 2008, **24**, 5253.

26 (*a*) P. Wang, S. M. Zakeeruddin, P. Comte, I. Exnar and M. Grätzel, *J. Am. Chem. Soc.*, 2003, **125**, 1166; (*b*) H. Yang, C. Yu, Q. Song, Y. Xia, F. Li, Z. Chen, X. Li, T. Yi and C. Huang, *Chem. Mater.*, 2006, **18**, 5173; (*c*) T. Katakabe, R. Kawano and M. Watanabe, *Electrochem. Solid-State Lett.*, 2007, **10**, F23.

27 K. Ueno, A. Inaba, M. Kondoh and M. Watanabe, *Langmuir*, 2008, **24**, 5253.

28 T. Nakashima and T. Kawai, *Chem. Commun.*, 2005, 1643.

29 V. Khare, A. Kraupner, A. Mantion, A. Jelicic, A. F. Thunemann, C. Giordano and A. Taubert, *Langmuir*, 2010, **26**, 10600.

30 M. W. Zhao, N. Li, L. Q. Zheng, G. Z. Li and L. Yu, *J. Dispersion Sci. Technol.*, 2008, **29**, 1103.

31 (*a*) F. L. Chen, I. W. Sun, H. P. Wang and C. H. Huang, in *Multi-Functional Materials and Structures, Pts 1 and 2*, ed. A. K. T. Lau, J. Lu, V. K. Varadan, F. K. Chang, J. P. Tu and P. M. Lam, 2008, pp. 1113–1116; (*b*) F. L. Chen, I. W. Sun, H. P. Wang, and C. H. Huang, *J. Nanomater.,*Volume 2009, Article ID 698501, 4 pages; 10.1155/2009/698501.

32 C. A. N. de Castro, M. J. V. Lourenco, A. P. C. Ribeiro, E. Langa, S. I. C. Vieira, P. Goodrich and C. Hardacre, *J. Chem. Eng. Data*, 2010, **55**, 653.

33 G. R. Patzke, Y. Zhou, R. Kontic and F. Conrad, *Angew. Chem., Int. Ed.*, 2011, **50**, 826.

34 S. G. Yang, T. Li, B. X. Gu and Y. W. Du, *Appl. Phys. Lett.*, 2003, **83**, 3746.

35 C. T. Hsieh, J. M. Chen, H. H. Lin and H. C. Shih, *Appl. Phys. Lett.*, 2003, **83**, 3383.

36 J. B. Reitz and E. I. Solomon, *J. Am. Chem. Soc.*, 1998, **120**, 11467.

37 A. MacDonald, *Nature*, 2001, **414**, 409.

38 A. Taubert, A. Uhlmann, A. Hedderich and K. Kirchhoff, *Inorg. Chem.*, 2008, **47**, 10758.

39 N. Liu, D. Wu, H. X. Wu, F. Luo and J. Chen, *Solid State Sci.*, 2008, **10**, 1049.

40 T. Alammar, A. Birkner and A. V. Mudring, *Eur. J. Inorg. Chem.*, 2009, 2765.

41 J. L. Ferguson, J. D. Holbrey, S. Ng, K. R. Seddon, A. A. Tomaszowska and D. F. Wassell, *Pure Appl. Chem.*, DOI: 10.1351/PAC-CON-11-07-21.

42 D. A. Shirley, *Phys. Rev.*, 1972, **B5**, 4709.

43 *CrysAlis PRO*. Agilent Technologies Ltd, 2010, Yarnton, England.

44 (*a*) G. M. Sheldrick, *Acta Crystallogr., Sect. A: Found. Crystallogr.*, 2008, **A64**, 112–122; (*b*) O. V. Dolomanov, L. J. Bourhis, R. J. Gildea, J. A. K. Howard and H. Puschmann, *J. Appl. Crystallogr.*, 2009, **42**, 339.

45 (*a*) G. Schön, *Surf. Sci.*, 1973, **35**, 96; (*b*) Y. C. Zhang, J. Y. Tang, G. L. Wang, M. Zhang and X. Y. Hu, *J. Cryst. Growth*, 2006, **294**, 278.

46 C. C. Chusuei, M. A. Brookshier and D. W. Goodman, *Langmuir*, 1999, **15**, 2806.

47 (*a*) E. Cano, J. M. Bastidas, J. L. Polo and N. Mora, *J. Electrochem. Soc.*, 2001, **148**, B431; (*b*) N. S. McIntyre, S. Sunder, D. W. Shoesmith and F. W. Stanchell, *J. Vac. Sci. Technol.*, 1981, **18**, 714; (*c*) Y. Wang, J. Liu and C. Xia, *Adv. Synth. Catal.*, 2011, **353**, 1534.

48 Y. Kikuchi, T. Suzuki and K. Sawada, *Bull. Chem. Soc. Jpn.*, 1990, **63**, 1819.

49 B. Liu, B. Liu, Y. Zhou and W. Chen, *Organometallics*, 2010, **29**, 1457.

50 N. Masciocchi, E. Corradi, A. Sironi, G. Morelli and P. Porta, *J. Solid State Chem.*, 1997, **131**, 252.

51 Y. Cudennec and A. Lecerf, *Solid State Sci.*, 2003, **5**, 1471.

52 J. Estager, P. Nockemann, K. R. Seddon, M. Swadzba-Kwasny and S. Tyrrell, *Inorg. Chem.*, 2011, **50**, 5258.

53 T. Weskamp, V. P. W. Böhm and W. A. Herrmann, *J. Organomet. Chem.*, 2000, **600**, 12; K. J. Cavell and D. S. McGuinness, *Coord. Chem. Rev.*, 2004, **248**, 671.